Results in Physics 7 (2017) 3222–3229

Contents lists available at ScienceDirect

Results in Physics

journal homepage: www.journals.elsevier.com/results-in-physics

Comparative studies of microstructural, tribological and corrosion properties of Zn-TiO_2 and Zn-TiO_2-WO_3 nano-composite coatings

A.A. Daniyan [a,*], L.E. Umoru [a], A.P.I. Popoola [b], O.S.I. Fayomi [b,c]

[a] Department of Materials Science and Engineering, Obafemi Awolowo University Ile-Ife, Nigeria
[b] Department of Chemical, Metallurgical and Materials Engineering, Tshwane University of Technology, P.M.B. X680, Pretoria, South Africa
[c] Department of Mechanical Engineering, Covenant University, P.M.B. 1023, Ota, Nigeria

ARTICLE INFO

Article history:
Received 19 May 2017
Received in revised form 3 August 2017
Accepted 28 August 2017
Available online 1 September 2017

Keywords:
Zn-TiO_2
Zn-TiO_2-WO_3
Electrocodeposition
Microstructure
Composite
Stability and coatings

ABSTRACT

Nano sized composites of Zn-TiO_2 and Zn-TiO_2-WO_3 were produced via electrocodeposition on plain carbon steel. The effect of input current on the microstructure, mechanical strengthening and corrosion properties were compared. The morphological features of the composite coatings were characterized by scanning electron microscope (SEM) equipped with energy dispersive spectrometer (EDS); mechanical properties were carried out using a diamond base Dura Scan hardness tester and CERT UMT-2 multi-functional tribological tester. The corrosion properties were investigated by potentiodynamic studies in 3.5% NaCl. The result showed that the coatings exhibited good stability and the particle loading of WO_3 greatly enhanced the microstructural properties, hardness behaviour and corrosion resistance of the coatings.

Introduction

Zinc is extensively used as metallic coatings applied to steel surfaces to shield them from corrosion which can be obtained either by hot dipping or electrodeposition process [1–5]. Electrolytic deposition of Zn generates thinner coating as compared to hot dipping method, which is suitable for the subsequent forming process in the automotive industries. With the selection of proper coating parameters, electrocodeposition can still give better coatings with fine surface finish that will exhibit high degree of corrosion resistance and mechanical properties such as microhardness, wear resistance, ductility, strength, decorative properties, etc. In spite of the fact that, zinc is anodic to steel, it protects the base steel even when the coating is porous [6,7]. However, high-quality deposition depends mainly on the nature of bath [8–11]. To improve zinc coating, a number of researchers have established the use of composite coating as advantageous alternative to ordinary zinc coating. Composite based coatings are progressively more used and the applications range from manufacturing to wear and hardness protection, corrosion resistance, and high temperature environments and several of these ceramics composites possess excellent bonds matrices with many functional coating particulates such as Zn-ZrO_2, Ni-SiC, Ni-ZrO_2, Ni-Al_2O_3, etc. [12,13]. However, when materials are reduced to nanoscale, they displayed distinctive properties that are quite different from what they exhibit in their bulk state, soft materials become hard, opaque materials become transparent, insulators turn to conductors, inert materials changed to reacting one and dielectrics becomes conductors [14,15]. Therefore, the use of nano-sized composite is of better performance and highly promising nowadays. Nanocomposite materials have various unique properties like excellent corrosion and wear resistance, resistance to high temperature oxidation, self lubricity, etc. [16].

Electrocodeposition method can yield porous-free finished products that do not require subsequent consolidation processing. Further this process requires low initial capital and provides high production rates with few shape and size limitations. Coating via electrodeposition have been considered to be one of the most viable techniques for fabricating nano-composite because of its low temperature operation, precise control, high rate of deposition and cost effectiveness [17]. Some authors have reported ZrO_2, TiO_2, Al_2O_3 and SiC particulates could be co-deposited along with metals or metallic alloys to form composite coatings [18–20]. Similarly, some alloys and composites such as Ni-W, Zn-ZrO_2 and Ni-W-SiC are developed as surface treatment to substitute for chromium coatings because of their excellent performance and environmental friendliness. WO_3 has been studied by a number of researchers

* Corresponding author.
E-mail address: daniyan03@gmail.com (A.A. Daniyan).

http://dx.doi.org/10.1016/j.rinp.2017.08.048
2211-3797/

as incorporation particulates for composite reinforcement; however the use of nanosized WO_3 for composite strengthening has received little attention. The need for phasing out chromium (Cr) coating because of its hazardous Cr (VI) product and other harmful coatings has been a global concern. Research findings have shown that one of the safe alternatives to this is the use of TiO_2 based coatings. Although, several attempts have been made to apply TiO_2 coatings for corrosion protection of metals, the problem of achieving an effective TiO_2 based coating system that can work effectively under dark and ultra violet conditions has been a challenge. There is a need to develop an effective and efficient active nano composite coating system on mild steel, using modified nano-TiO_2 coatings in zinc matrix via electrocodeposition route. Therefore in this study, microstructural, mechanical reinforcement and corrosion resistance properties of Zn-TiO_2 and Zn-TiO_2-WO_3 which are better and save alternatives to chromium coating prepared via electrocodeposited through chloride bath are comparatively studied.

Experimental procedure

Substrate preparation

The dimension of the steel (substrate) used was (45 × 40 × 20) mm^3 sheet and zinc sheets of (85 × 45 × 5) mm^3 were prepared as anodes. The mild steel specimens' chemical composition is shown in Table 1. The cathode was mild steel samples (coupons) and anode of pure zinc (99.99%). The mild steel specimens were polished mechanically, degreased and rinsed with water as described by [21,22].

Coating formation

The mild steel substrate earlier prepared was activated by dipping into 10% HCl solution for about 10 s followed by rinsing in deionized water. Analar grade of chemicals and deionized water were used for preparation of the coating solution at room temperature before plating. The bath formulations were prepared a day before and stir continuously at the rate of 400 rpm with constant heating at 70 °C throughout the plating process, to obtain dispersion stability of particles in the solution [23,24]. The bath compositions used for the different coating matrix are as follow; 120 g/l of $ZnCl_2$, 30 g/l of KCl, 20 g/l of TiO_2 nano particles, 15 g/l of WO_3 nanoparticles, 0.5 g/l of 2-Butyne-1,4-diol, 0.5 g/l of Cetylpridinium Chloride and 10 g/l of Thiourea.

The selection of the deposition parameter is in agreement with the study from previous work of some of our group [20]. The prepared zinc electrodes were connected to the rectifier at varying current between 1.0 A (current density of 560 A/m^2) and 1.5 A (current density of 830 A/m^2) for 20 min constant time (Table 2). The table displayed the deposition results from the electrocodeposition bath of the nanocomposites. The appreciable increase of the weight and coating thickness can be traceable primarily, due to increase in the current density, though other parameters like favourable temperature, pH, etc. are also germane [20]. The coated samples were rinsed in water and air-dried. Thereafter, the coated steel samples were sectioned into parts for characterization.

Characterization of coating

The nano-composite coatings obtained were characterized with JEOL FIELD EMMISSION JSM – 7600F, Scanning electron microscope attached with EDS. Micro-hardness evaluations were carried out using a diamond pyramid indenter EMCO Test Dura-scan 10 micro-hardness testers at a load of 10 g for a period of 20 s. The micro-hardness was measured across the plated surface.

Friction and wear tests

The tribological properties of the composite coating were characterized using CERT UMT-2 multi-functional tribological tester at ambient temperature of 25 °C (the schematic diagram is shown in Fig. 1). The reciprocating sliding tests was carried out with a load of 5 N, constant speed of 5 mm/s, displacement amplitude of 2 mm in 20 min. A Si_3N ball (4 mm in diameter, HV 50g-1600) was chosen as counter body for the inspection of tribological behaviour of the coated sample. The dimension of the wear specimen is about 2 cm by 1.5 cm as prescribed by the specimen holder. After the wear test, the structure of the wear scar and film worn tracks are further examined with the help of high optic Nikon Optical microscope (OPM) and scanning electron microscope equipped with energy dispersive spectroscopy (JEOL FIELD EMMISSION SEM/EDS).

Electrochemical test

The electrochemical studies were performed with Autolab PGSTAT 101 Metrohm Potentiostat using a three-electrode cell assembly in a 3.5% NaCl static solution at room temperature. The developed composite was used as the working electrode, a platinum electrode was used as counter electrode and Ag/AgCl was used as the reference electrode.

Table 1
Elemental analysis of the mild steel used.

Element	% Content	Element	% Content	Element	% Content
C	0.134	Mo	0.083	Ti	<0.002
Si	0.119	Ni	0.019	V	0.0048
Mn	0.237	Cu	0.044	W	0.024
P	<0.003	Al	0.050	B	>0.016
S	>0.156	Co	0.012	Sn	0.0046
Cr	0.094	Nb	<0.005	Fe	97.70

Table 2
Formulation designed bath composition for Zn-TiO_2/Zn-marinTiO_2-WO_3 nano-composites.

Matrix sample	Time of deposition (min)	Thickness of the coating (μm)	Weight gained (g)	Current density (A/cm^2)	Plating per unit area (g/cm^2)
Zn-20TiO_2	20	20	0.43	560	0.026
Zn-20TiO_2	20	25	0.53	830	0.028
Zn-20TiO_2-15WO_3	20	35	0.41	560	0.023
Zn-20TiO_2-15WO_3	20	40	0.51	830	0.036

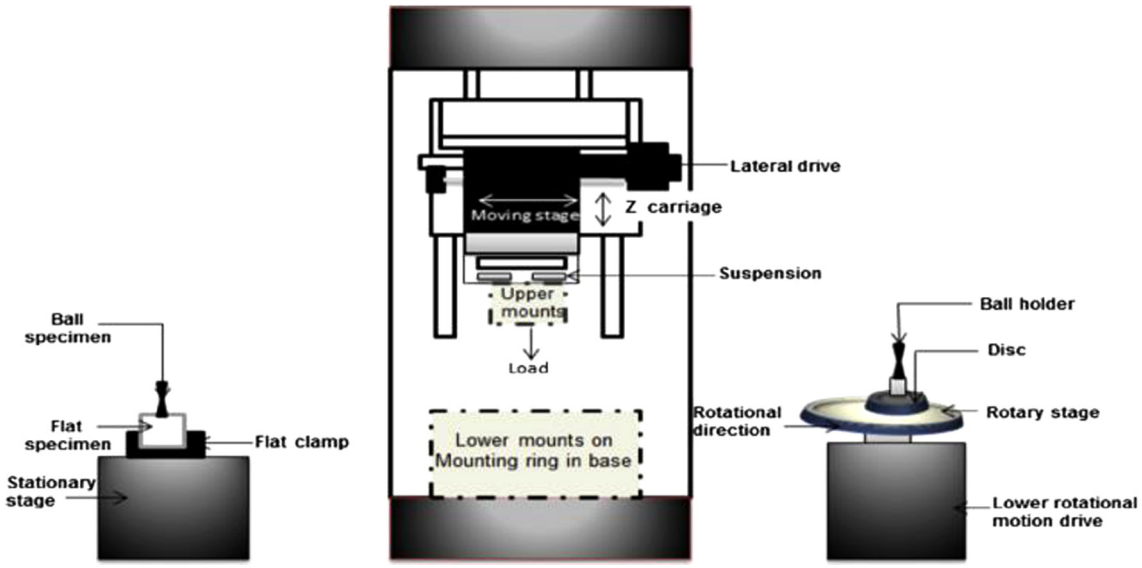

Fig. 1. Schematic view of reciprocating sliding friction CERT UMT-2 test system [11].

Results and discussion

Morphological studies

Fig. 2 shows the SEM/EDS structures of Zn coating on the mild steel at 830 A/cm^2 while Figs. 3 and 4 show the SEM/EDS structures of Zn-TiO_2 and Zn-TiO_2-WO_3 nano-composites matrixes at 1.5 A (830 A/m^2 current density) respectively deposited on mild steel. From the two figures it is obvious that the crystallites of the deposits are homogeneously distributed on the surfaces. It is clear that the structure of Zn-TiO_2 nanocomposite coating shows some flaky morphology, though still better than the Zn coating (Fig. 1) due to the presence of TiO_2 nanoparticulate in the Zn matrix. Nevertheless, the incorporation of WO_3 nanoparticles has caused a noticeable crystallite of the composite nodules along the interface Zn-TiO_2 nanocomposite. In fact there are two distinctive phases, the first having a homogeneously identical steady precipitate and the latter with network of agglomerate nodules. Obviously, the incorporation of the WO_3 along the zinc interface could be evident to give refined morphology with finer nodular particles. These networks of nodular structure of the Zn-TiO_2-WO_3 nanocomposite were more pronounced at 1.5 A (830 A/m^2) compared to at 1.0 A (560) (Fig. 5). This further emphasized the importance of current density in electrocodeposition and more so, particles' codeposition increases with current density [25].

The coating appearance and the plating interface of Zn-TiO_2-WO_3 are quite attractive and adherent because of the presence of TiO_2 and WO_3 nano ceramics particulates that synergistically fortified the composite. The structure was as expected since the process of nucleation initiated from the zinc metal as load carrier, the distribution of the particulates covers the nucleation points and enhanced the produced composite [25–29]. Moreover, it is important to mention that the morphological change may be due to the presence of WO_3 particles incorporated in the composite leading to improved precipitation and better strengthening. Also, according to [30], the current induced coupled with other coating parameters

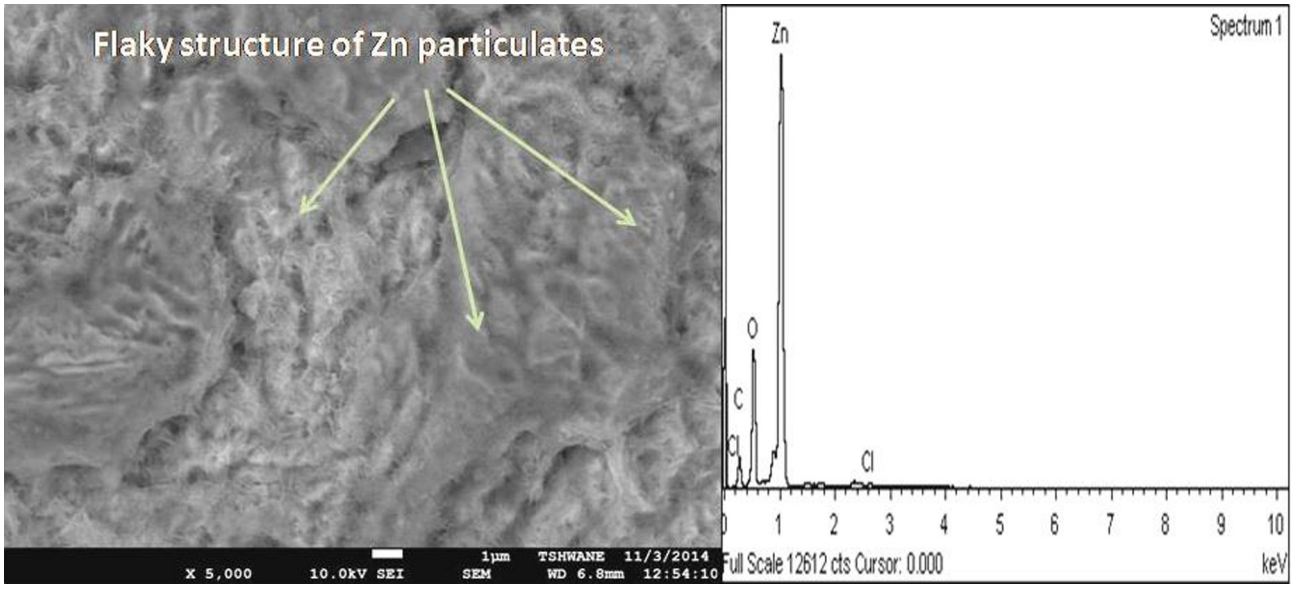

Fig. 2. SEM/EDS of Zn coated mild steel at 830 A/cm^2 showing the surface morphology.

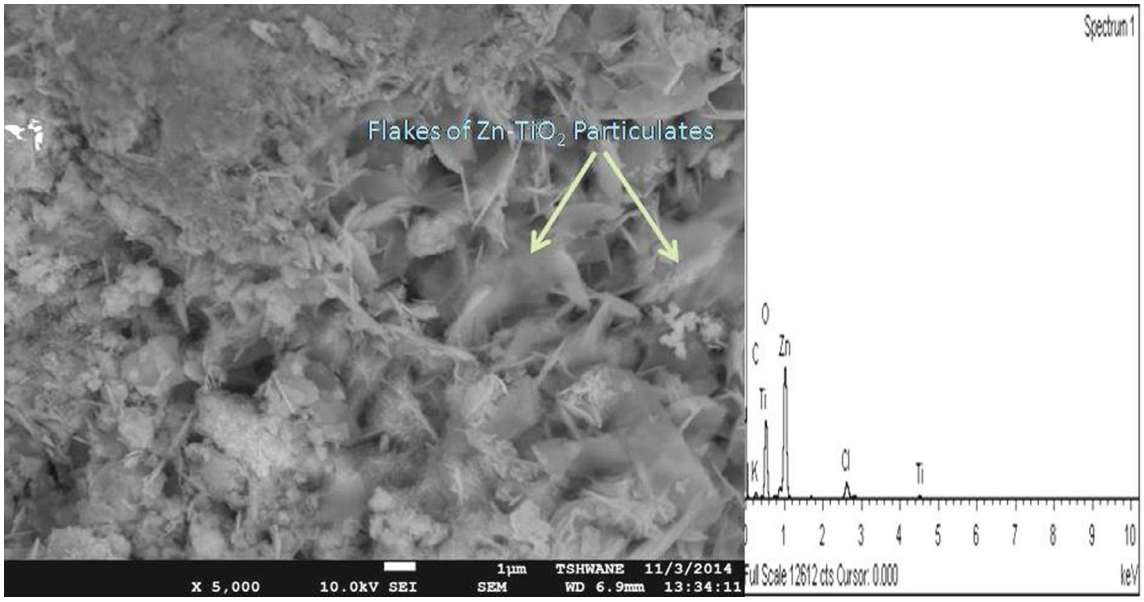

Fig. 3. SEM/EDS of Zn-TiO_2 coated mild steel at 830 A/cm^2 showing the surface morphology.

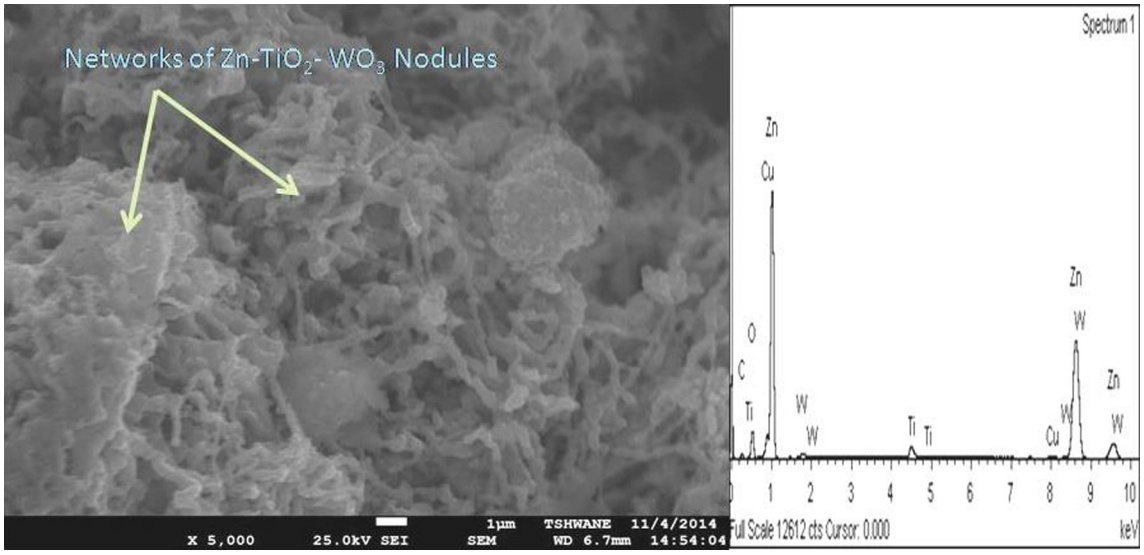

Fig. 4. SEM/EDS of Zn-TiO_2-WO_3 coated mild steel at 830 A/cm^2 showing the surface morphology.

with respect to the quantity of additive can also play a very significant role in modification of the crystal direction and surface quality of a deposited material.

Microhardness study

The microhardness assessment shown in Fig. 6 was done so as to observe the effect of the composite microstructure and its particle loading on the hardness behaviour of Zn-TiO_2 and Zn-TiO_2-WO_3 nanocomposite coatings. Therefore, some specimens were prepared for microhardness tests.

Generally, all the nano-composites produced, display excellent and unique improvement compared to the uncoated mild steel substrate, which could be traced to the effect of nano-sized particulate loading. However, the sample matrices of Zn-TiO_2-WO_3 showed the higher hardness property with the optimal performance at 1.0 A. The outstanding enhancement of these matrices is primarily due to microstructural strengthening of WO_3 loaded into the Zn-TiO_2 matrix. Though the hardness decreased as the applied current was increased from 1.0 A to 1.5 A. This reduction in hardness could be influenced by the anomaly that occurred as can be explained from Faraday first law of electrolysis. Factors such as, operating conditions, composition of electrolyte and diffusion mechanism could influence the result [31,32]. Fig. 7 revealed the effect of the composite coating to the heat treatment. The thermal deformations were observed in 250 °C for 5 h and mechanical responses of the plated samples were examined. It is obvious that heating the samples did increase the hardness properties of the samples, except Zn-TiO_2-WO_3-1.5A matrix which reduced from 153 HVN to 137 HVN. This could be traced to variation in co-deposition parameters. Nevertheless, the coating did not experience any crack or flaw at the interface but a kind of grain refinement. The mechanical behaviour due to thermal treatment and porosity within the composite surface could result in hardness distribution. Some literatures also agree to the fact that compression stress could significantly perk up the micro-hardness when it is

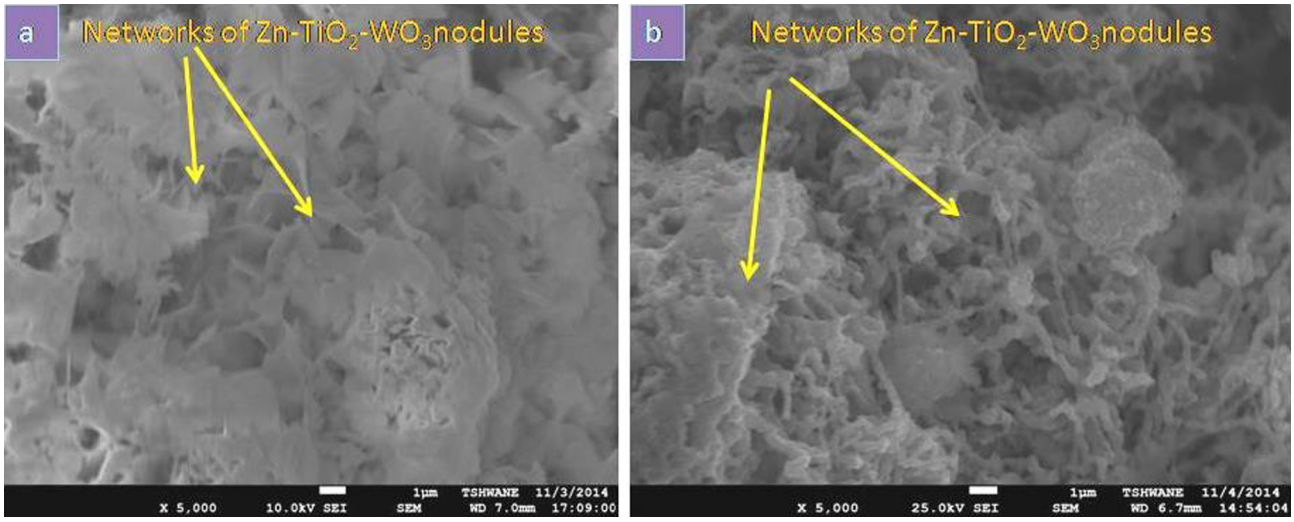

Fig. 5. SEM/EDS of Zn-TiO_2-WO_3 coated mild steel at (a) 560 and (b) 830 A/cm^2 showing the surface morphology.

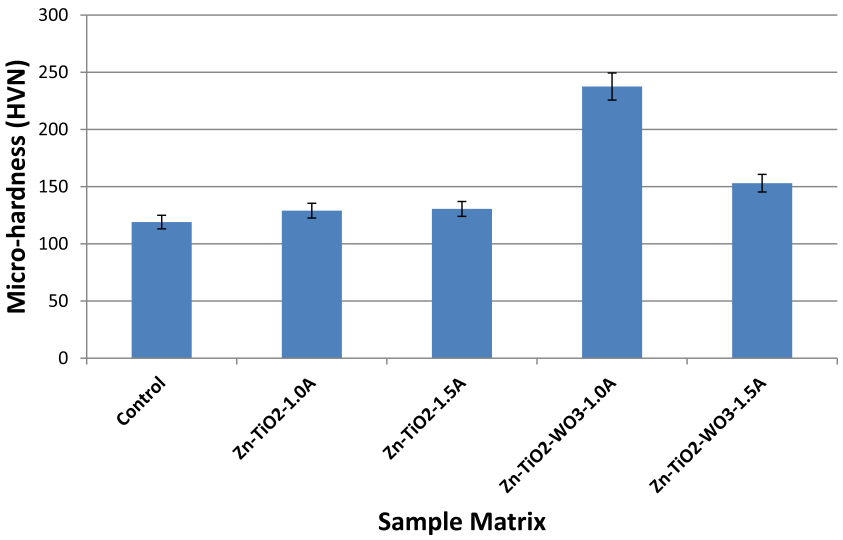

Fig. 6. Hardness properties of varied current of Zn-TiO_2-WO_3 nano-composite deposited on mild steel before heat treatment.

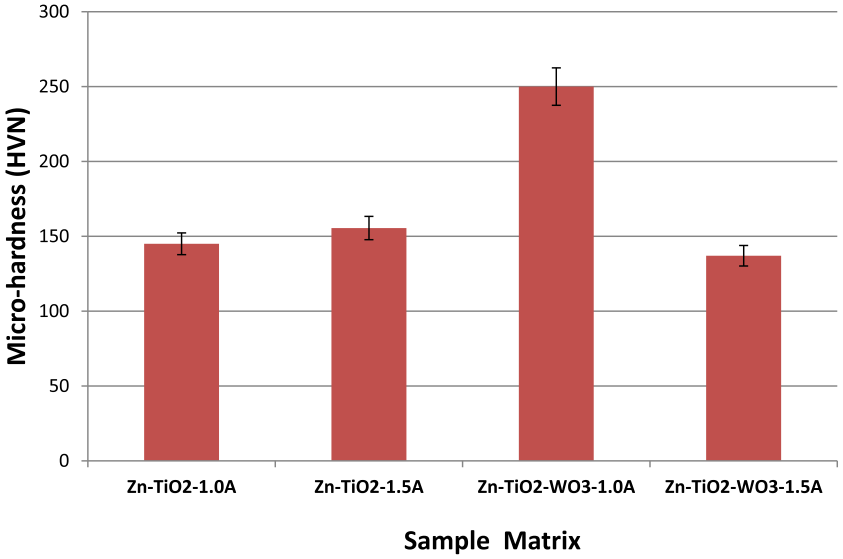

Fig. 7. Hardness properties of varied current of Zn-TiO_2-WO_3 nano-composite deposited on mild steel after heat treatment.

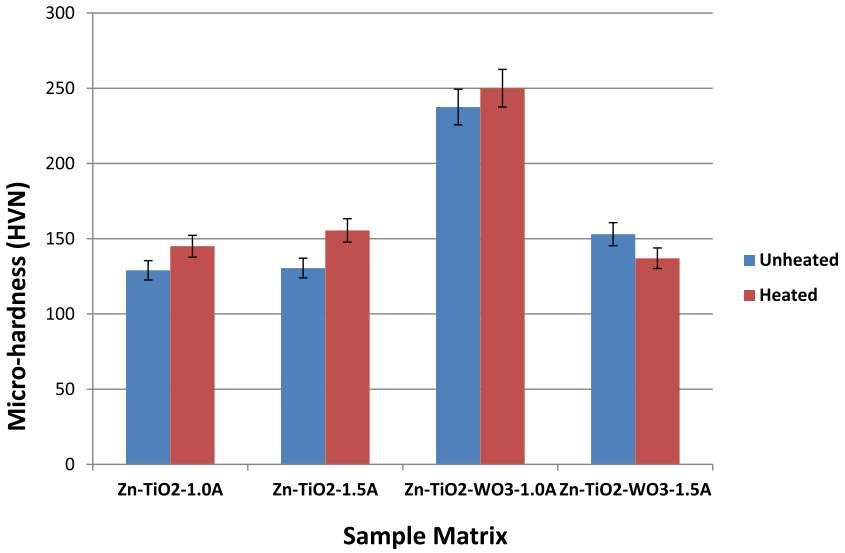

Fig. 8. Microhardness variation of the nano-composite coating before and after heat treatment.

much less than the ultimate strength of the coating but it has been revealed [25,33,34] that the flaws such as porosity, macro-particle at the composite surface will have unfavourable effect on the mechanical properties. Fig. 8 compare the hardness properties of the composite coatings before and after thermal treatment. The average micro hardness values for all the samples calculated indicates that, Zn-TiO_2-WO_3-1.0A nanocomposite coatings possessed the highest value of hardness (237.5 HVN), increased to 250 HVN after heat-treatment and still maintained its optimal value. It can also be observed from Fig. 8 that, the hardness after heat treatment increases from 129 to 145 HVN and 130 to 155.5 HVN before the incorporation WO_3. The coatings were excellent since the hardness values after heating were still maintained more than 50% of their values before thermal treatment [20]. The phenomenon of dispersion strengthening was also observed. The mechanisms of such strengthening are the grain refinement strengthening and the dispersion strengthening of WO_3 deposited on the sample and the deposition current [17,18]. In general the enhancement in hardness could be attributed to the development of adhesive properties on the substrate coupled with difference phases formed and the microstructural refinement of grains.

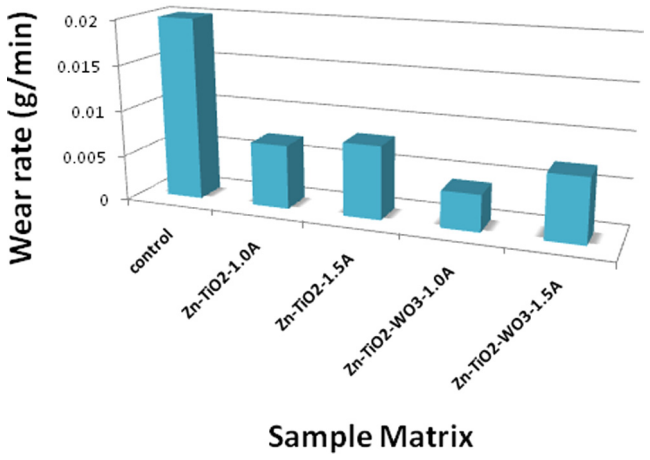

Fig. 9. Variation of wear rate with time.

Wear analysis of the composite coating on mild steel

Fig. 9 shows the wear loss of difference sample matrices of Zn-TiO_2 and Zn-TiO_2-WO_3 nanocomposite coatings. It is clear that all the nanocomposite coatings exhibited higher wear resistance than the control (unplated sample). Obviously, it can also be further seen that, the wear loss of Zn-TiO_2 matrices are higher than of the Zn-TiO_2-WO_3. Meaning that the latter exhibited a higher wear resistance than the former, as it is clearly noticed that Zn-TiO_2-WO_3-1.0A displayed the best wear resistance. Thus the addition of WO_3 in the matrix has immensely contributed to the enhanced wear resistance. This can be ascribed to the strengthening effect of WO_3 nanoparticulate loading. The process parameter of hardness and microstructural performance are the factors which affect the wear resistance [18,19]. The nanocomposite coatings of Zn-TiO_2-WO_3-1.0A showed the least tendency for plastic deformation. With reference to [20], the incorporated WO_3 particles can significantly improve the tribological performance of Zn-TiO_2-WO_3 nanocomposite coating.

Fig. 10 shows the microscopic examination of worn surfaces of the coated samples of Zn-TiO_2 and Zn-TiO_2-WO_3 at varying current. From the scar, plastic deformation and grooves can be seen on the surfaces of the samples as shown. The impact of reciprocating sliding disc was very high on the substrates as the penetration lead to visual stress though with no fracture. The coated sample Zn-TiO_2-WO_3-1.0A showed the best appearance, slightest visible plastic deformation and distinctive networks of worn tracks which are in agreement with the result in Fig. 8. Obviously, the embedded conditioned composite matrix could have been responsible for this wear resistance especially with the presence of TiO_2 and WO_3. Shibli et al. [21], testified in their preliminary literature of composite studies that mixed oxide formed can provide tremendous wear resistance properties. Because of this unnoticed plastic deformation of composite coatings is a strong indication of the early report that the development of oxide films on the worn surfaces of these nanocomposites provides a superior wear resistance as expected. It is worth noting that no severe fracture in all the samples. Furthermore, the continuous slide in coefficient of friction during wear mechanism could reduce plastic deformation of the sample with Zn-TiO_2-WO_3-1.0A exhibited the least coefficient of friction in accordance to [21,22].

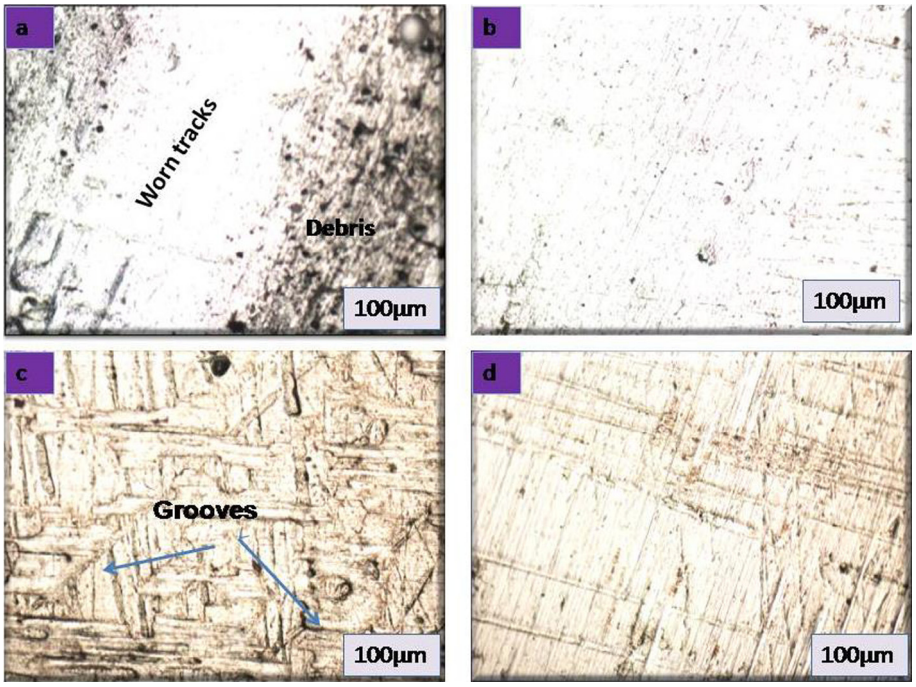

Fig. 10. Micrographs of the wear scar for (a) Zn-TiO_2-1.0A, (b) Zn-TiO_2-1.5A, (c) Zn-TiO_2-WO_3-1.0A, (d) Zn-TiO_2-WO_3-1.5A deposited sample.

Polarization measurements

Table 3 presented the extrapolated values of E_{Corr}, I_{Corr}, corrosion rate (CR) and polarization resistance (R_P) of the samples from Tafel slope. The results showed the corrosion resistance behaviour of the coatings in 3.5% NaCl static solution at constant scan rate. From the Potentiodynamic polarization curves of Zn-TiO_2 and Zn-TiO_2-WO_3 nano composite coatings in Fig. 11, it was established that the addition of WO_3 nano-particulate changed the shape of the polarization curve but causes a significant increase in the value of the E_{corr}. These characteristics indicate that an increase in the quantities of additive improve this process. It is also clear from the polarization curve that the Zn-TiO_2-WO_3 matrices displayed higher polarization potential. Meaning that, they have better corrosion resistance than the Zn-TiO_2 series and the best value for the coating with least corrosion rate was Zn-TiO_2-WO_3-1.5A, which implies that addition of WO_3 provides better effect of corrosion resistant property, This could be attributed to the nature and tenacity of the passive film produced by Zn-TiO_2-WO_3-1.5A on the surface of the coated steel. Noticeably, improvement in potential was discovered appreciably for all coatings, which could be attributed to the coatings effect of the film precipitated at the interface of the Zn matrix [25]. Unlike the uncoated substrate that possesses less passive film formed on the surface, which results into severe corrosion attack of the chloride solution having a polarization potential of about −1.4 V which below that of the coated species. The coating properties of all the coating were unique. The summary of the results for the polarization measurements are shown in Table 3 which were obtained from Tafel plots and the drop in the potential thereafter could be traced to slight passivity breakdown experienced when the concentration of WO_3 was further increased [26]. Fig. 12 shows the morphologies of the composite coating before and after corrosion tests in the accelerated chloride solution. Corrosion products of general type and localized pits occurred on the mild steel uncoated substrate while uniform corrosion was only seen on all the surfaces of Zn-TiO_2 and Zn-TiO_2-WO_3 coated surfaces. TiO_2-rich intermetallic particles and

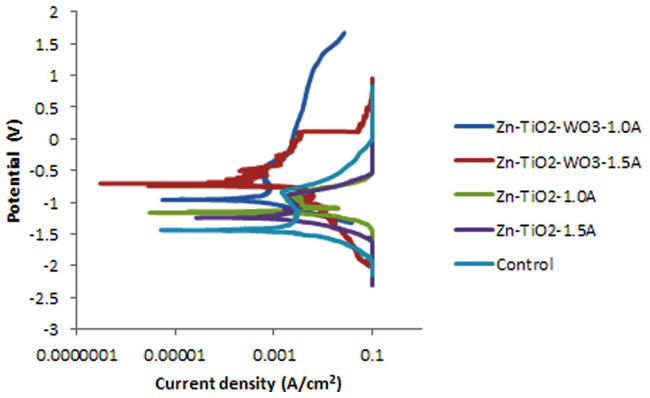

Fig. 11. Potentiodynamic polarization curves of Zn-TiO_2/Zn-TiO_2-WO_3 composite coatings on mild steel in 3.5% NaCl solution.

Table 3
Polarization data extrapolated from Tafel slope for matrix Zn-TiO_2-WO_3 composite coating.

Sample in 3.5% NaCl	E_{corr} (V)	j_{corr} (A/m^2)	Corrosion rate (mm/year)	Polarization resistance (Ω)
Control	−1.43921	0.005083	1.9566	18.037
Zn-TiO_2-1.0A	−1.16547	0.002056	0.79144	31.706
Zn-TiO_2-1.5A	−1.2442	0.003015	1.1606	25.362
Zn-TiO_2-WO_3-1.0A	−0.968628	0.000934	0.35964	41.524
Zn-TiO_2-WO_3-1.5A	−0.70462	0.000263	0.10116	99.428

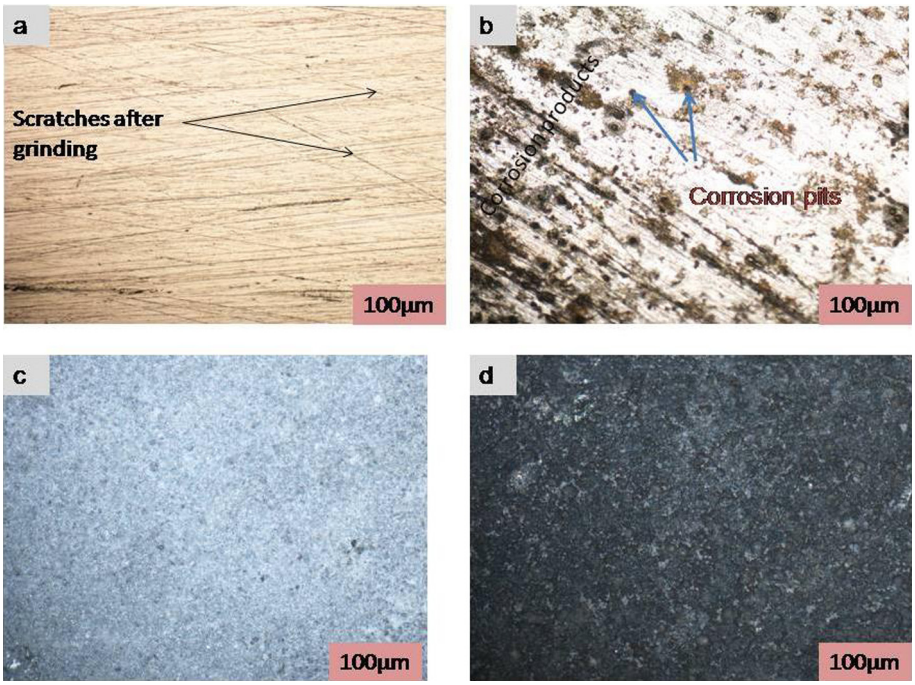

Fig. 12. Micrographs of the uncoated (control) samples (a) before corrosion (b) after corrosion (c) Zn-TiO_2 coated (d) Zn-TiO_2-WO_3 coated samples after.

incorporation of WO_3 Nanoparticulate mitigate corrosion and promote cathodic reduction reactions.

Conclusion

1. Nano structured TiO_2 and WO_3 particulates were used to generate Zn-TiO_2/Zn-TiO_2-WO_3 nano-composite coating from chloride bath.
2. The incorporation of TiO_2 and WO_3 in the coatings was confirmed by EDX.
3. Zn-TiO_2-WO_3 nano-composite exhibited higher microhardness, higher wear resistance and better corrosion resistance compared to that of Zn-TiO_2 but both nano-composites displayed far better properties than the uncoated substrate.
4. The incorporation of the TiO_2/WO_3 Nanoceramics composite particles in the zinc matrix as strengtheners boosted the hardness properties. The hardness properties increase with increase in particulate incorporation.
5. The enhancement of the corrosion resistance may be due to physical barriers offered by TiO_2 and WO_3 to the corrosion process by filling crevices and minute holes on the surface of the composite coating.

Appendix A. Supplementary data

Supplementary data associated with this article can be found, in the online version, at http://dx.doi.org/10.1016/j.rinp.2017.08.048.

References

[1] Basavanna S, Arthoba Naik Y. J Appl Electrochem 2009;39:1975.
[2] Hague IU, Ahmad N, Akhan A. J Chem Soc Pakistan 2005;27:337.
[3] Popoola API, Fayomi OS. Int J Electrochem Sci 2011;6:3254.
[4] Rahman MJ, Sen SR, Moniruzzaman M, Shorowordi KM. J Mech Eng Trans 2009;40:9.
[5] Volinsky AA, Vella J, Adhihetty IS, Sarihan VL, Mercado L, Yeung BH, et al. Mater Res Soc 2001;649:1.
[6] Shivakumara S, Manohar U, Arthoba Naik Y, Venkatesha TU. Bull Mater Sci 2007;30.
[7] Panagopoules CN, Tsoutsouvaa MG. Corros Eng Sci Technol 2011;46:513.
[8] Pedroza GAG, Souza CAC, Carlos IA, Andrade Lima LRP. Surf Coat Technol 2012;206:2927.
[9] Mohankumar C, Praveen K, Venkatesha V, Vathsala K, Nayana O. J Coat Technol Res 2012;9(1):71.
[10] Mou C, Sen Sen X, Ming Y. J Solid State Electrochem 2010;14:2235.
[11] Basavanna S, Arthoba Naik Y. J Appl Electrochem 2009;39:1975.
[12] Byk TV, Gaevsaya TV, Tsybulskaya A. Surf Coat Technol 2008;202:5817–23.
[13] Chitharanjan HA, Venkatakrishna K, Eliaz N. Surf Coat Technol 2010;205:2031.
[14] Afonja AA. Niger J Mater Sci Eng 2009;1(1):63.
[15] Daniyan AA, Umoru LE, Fasasi AY, Borode JO, Oluwasegun KM, Olusunle SOO. J Miner Mater Charact Eng 2014;2.
[16] Ger MD, Grebe R. Mater Chem Phys 2004;87:67.
[17] Kwok CT, Cheng FT, Man HC. J Surf Coat Technol 2006;200:3544.
[18] Popoola API, Pityana SL, Popoola OM. J South Afr Inst Min Metall 2011;111:345.
[19] Noor EA, Al-Moubaraki AH. Int J Electrochem Sci 2008;3:806.
[20] Popoola API, Fayomi OS. Int J Phys Sci 2011;6:2447.
[21] Shibli SMA, Chacko F, Divya C. J Corros Sci 2010;52:518.
[22] Fayomi OSI, Popoola API. Res Chem Intermed Res 2013;39:N06. http://dx.doi.org/10.1007/s11164-013-1354-2. ISSN: 0922-6168.
[23] Hunter RJ. Foundations of colloid science. 2nd ed. Oxford, New York: Oxford University Press; 2001.
[24] Myers D. Surfaces, interfaces and colloids – principles and applications. 2nd ed. New York: Wiley-VCH; 1999.
[25] Fayomi OSI, Loto CA, Popoola API, Tau V. Int J Electrochem Sci 2014;9:7359.
[26] Wang SL, Murr LE. J Metallogr 1980;13:203–24.
[27] Byk TV, Gaevsaya TV, Tsybulskaya A. Surf Coat Technol 2008;202:5817–23.
[28] Chitharanjan HA, Venkatakrishna K, Eliaz N. Surf Coat Technol 2010;205:2031–41.
[29] Nayana KO, Venkateshe TV, Praven BM, Vathsala K. J Appl Electrochem 2011;41:39–49.
[30] Praveen BM, Venkatesha TV. Appl Surf Sci 2008;254:2418–24.
[31] Dikici T, Culha O, Toparli M. J Coat Technol Res 2010;7:787–92.
[32] Byk TV, Gaevsaya TV, Tsybulskaya A. Surf Coat Technol 2008;202:5817–23.
[33] Chitharanjan HA, Venkatakrishna K, Eliaz N. Surf Coat Technol 2010;205:2031–41.
[34] Popoola API, Fayomi OS. Sci Res Essay 2011;6:4264–72.